Water Air Soil Pollut (2023) 234:250
https://doi.org/10.1007/s11270-023-06238-3

The Potential of *Moringa oleifera* Seed in Water Coagulation-Flocculation Technique to Reduce Water Turbidity

Farouk Abdullah Rasheed · Karwan Alkaradaghi · Nadhir Al-Ansari

Received: 30 December 2022 / Accepted: 8 March 2023 / Published online: 3 April 2023

Abstract Using a safe and easy-to-apply economic flocculant to replace alum is necessary to expand and enhance the water quality in rural regions where traditional water treatment is unavailable. The seed of *Moringa oleifera* is locally available in large volumes and is feasibly economical. A compatibility and applicability research of the easily accessible local *Moringa oleifera* seed extract (MOSE) was conducted to examine its potential utilization to lessen various degrees of water turbidity at 30 ± 2 °C. The study concerns the optimum dosage of MOSE to give high turbidity removal efficiency in the water. Experiments were carried out for nine turbidity samples: 5, 10, 15, 30, 50, 70, 100, 200, and 300 NTU. The turbidity removal efficiency of up to 89% was achieved for high initial turbid water 300 NTU. However, for low turbid water, its potential efficiency declined. The results demonstrate that the de-oiled extract is substantially more efficient than the crude extract in agglomerating colloidal particles of low initial turbidity samples and achieved up to 76% removal rate. The results of the ANOVA confirmed that the regression model was significant at ($p < 0.05$) for residual turbidity after the treatment process. The study also demonstrates that a pseudo-first-order kinetic model matched well the nature of the removal of colloidal particles with MOSE in water to form flocs. The study also indicates that the characteristics of water treated with crude MOSE produce little change in electrical conductivity and salinity. However, the hardness and alkalinity of water decreased significantly depending on the initial hardness and the amount of MOSE applied ($p < 0.05$).

Keywords *Moringa oleifera* seed · Turbidity · Coagulation · Flocculation · Water quality · Removal efficiency

F. A. Rasheed
Department of Water Resource, College of Engineering, University of Sulaimani, 460013 Sulaymaniyah, Iraq
e-mail: Farouk.rasheed@univsl.edu.iq

K. Alkaradaghi · N. Al-Ansari (✉)
Lulea University of Technology, 971 87 Lulea, Sweden
e-mail: nadhir.alansari@ltu.se

K. Alkaradaghi
e-mail: alkaradaghi.karwan@gmail.com

K. Alkaradaghi
Kurdistan Institution for Strategic Studies and Scientific Research, Sulaimaniyah 460013, Iraq

1 Introduction

The availability of high-quality freshwater with low turbidity is the most fundamental issue due to potential interaction with downstream treatment operations and negative impacts on customer acceptability (Mohseni-Bandpei et al., 2018). The turbidity of surface water changes according to the year's season, mainly from agriculture and development activity, with high erosion rates due to silt and clay that can carry substantial amounts of pollutants (Igwe et al.,

2017) (Razali et al., 2020). Water turbidity causes limited sunlight penetration into water bodies. Thus, it can harm fish and other aquatic life by reducing food supplies, degrading spawning beds, and affecting gill function (Matta et al., 2017).

Undesirable water turbidity not only causes public health problems but also creates an inadequate budget for water treatment processes because the safe drinking water supply should be free of turbidity (Anthony et al., 2021). Therefore, intake water from lakes and rivers should pass through treatment techniques to make it harmless and attractive to the consumers. Proper treatment is vital before usage (Kurniawan et al., 2012). The type of water treatment depends on the residue present in the water (Cui et al., 2020).

Various conventional methods, such as precipitation, adsorption, flotation, ion exchange, membrane filtration, and biological and electrolytic process, have been utilized to reduce and remove turbidity from water (Rajoria et al., 2022). Coagulation and flocculation are fundamental units in surface water treatment. Coagulation is the addition of synthetic or natural coagulants into the water to destabilize the negative charges of colloidal particles (Bhatia et al., 2007). Flocculation is a slow, gentle mixing of water to advance the flocs to grow to a bigger size to settle out quickly (Nan et al., 2016). Removing minute colloids depends on the amount of coagulant added.

Aluminum sulfate is the most widely used coagulant in water treatment because of its proven capability and lower cost. However, it creates by-products that harm human health (Wu et al., 2012); (Elsayed et al., 2021). Low-cost and safe coagulants with high cation capability are required to avoid this issue. Research in the past four decades has increasingly been directed toward producing natural coagulants that are renewable and nontoxic (Mumbi et al., 2018). The coagulant of *Moringa oleifera* seed extract (MOSE) is an alternative and is commonly used in less developed communities since it is easily biodegradable (Yamaguchi et al., 2021). The MOSE is feasible and applicable in separating colloidal particles because the extract components contain soluble cationic proteins, peptides, calcium, iron, vitamin C, and tocopherol that functions as a cationic polyelectrolyte (Dzuvor et al., 2022). Furthermore, the volume of settled sludge produced during the process can be used as bio-fertilizers to increase crop rates (Idris et al., 2016).

The rural communities in Iraq have freshwater scarcity. These areas suffer from conventional water treatment to treat seasonal variations in turbidity. Moreover, residents lack the expertise to remediate water quality using alum coagulants. Failure to use the alum dosage might cause Alzheimer's disease. The use of MOSE is developed and expected to provide more advantages and is reported as low cost and safe to be consumed.

The research aims to utilize a safe and easy application of a low-cost natural coagulant of MOSE as a replacement for alum coagulant to evaluate and improve the water quality the residents in rural communities use for drinking water. The research focuses on the detailed dosage knowledge to treat various raw turbid water entering the areas. The study also gives clear instructions on how the dosages of MOSE (oiled and de-oiled) can neutralize and destabilize the suspension charge of turbid water and make water suitable for a drink.

2 Methodology

2.1 Water sample Preparation

Raw water turbidity samples ranging from 5–300 NTU were prepared using an ordinary China kaolin clay powder obtained from Chemical Drug House. A weight of 10 g of kaolin powder was suspended in a liter of tap water using a magnetic stirrer for half an hour to attain a homogenous raw sample. The kaolin suspension was allowed to settle down for more than an hour. Only supernatant is used for the coagulation experiments. Thus, colloidal particles are observed in water and used as a stock solution to prepare desirable turbid water samples after dilution practice. Prepared turbid water was kept and filled into clean 1.5-L polyethylene terephthalate bottles, and its turbidity was measured before coagulant addition.

2.2 Physiochemical Measurements of *M. oleifera* Coagulant

This research was carried out at the beginning of June month of 2021. The dried *M. oleifera* pods were collected from the Bakrajo agriculture field in Sulaymaniyah, Iraq (35°33′02.5″ N 45°20′27.1″ E). The coats and wings were removed and then crushed to a fine powder using a crusher and then sieved through a 250-µm sieve. To make the MOSE solution, 2 g of the seed was weighed and dissolved in 200 ml of distilled water in a beaker, followed by an hour of stirring and filtering through Whatman filter paper No. 42. To make de-oiled MOSE, 2 g of powdered seed was combined with 100 ml of 70% n-hexane as an extract solvent for 40 min. Subsequent separation of the residue from the supernatant occurred by centrifuging for 45 min at 4000 rpm. The supernatant was discarded, and the residual solid was dried at room temperature. From the dried sample, 2 g was mixed with 200 ml of distilled water. The suspensions were stirred for 40 min. The supernatant was filtrated through Whatman filter No. 1 after leaving the mixture to sediment totally. The filtrate was considered the de-oiled extract.

2.3 Coagulation Experiments

The experimental tests were implemented using a jar test apparatus coupled with six paddles (Model/ Wagtech project, EN/ 15–810, Code/ F105AD109), as shown in Fig. 1. The beakers were well-washed and filled with a 1000-ml raw water sample after knowing its initial turbidity. The temperature of the water samples was 30 ± 2 °C. Different dosages 5–240 mg. L^{-1} of the extract was used for low, medium, and high typical initial turbid samples to obtain the optimum dosage required for turbidity removal. The jar apparatus underwent rapid mixing with the speed of 110 rpm for 1.5 min and then a slow mixing speed of 25 rpm for 25 min. Later, the suspensions were left for 30 min to settle down the floc formations in the beakers. The supernatants in beakers were collected for turbidity measurements from 20 cm beneath the water surface in each beaker using a pipette. The turbidity of water samples was measured as Nephelometric Turbidity Units NTU using the turbidimeter (Hanna turbidity meter HI93703). Each experiment run was performed twice to ensure the results' accuracy.

The value of pH, electrical conductivity, alkalinity, and hardness before and after treatment was measured. Figure 2 illustrates the process steps of coagulation for treating raw water samples with turbidity 100 NTU. The performance efficiency removal of MOSE coagulant was determined using the following equation:

$$\%\ \text{Performance efficiency} = \frac{\text{Initial turbidity(NTU)} - \text{Residual turbidity(NTU)}}{\text{Initial turbidity(NTU)}} * 100 \tag{1}$$

Equation (1) does not take into account the decrease of turbidity in the negative control. The natural sedimentation of synthetic turbid samples in the absence of MOSE for 60 min was examined to show the natural settlement of colloidal particles in tap water and the main residual turbidity in the supernatant. One liter volume of synthetic initial turbidity samples of 5, 10, 15, 30, 50, 70, 100, 200, and 300

Fig. 1 Jar test—coagulation and flocculation process for surface water turbid

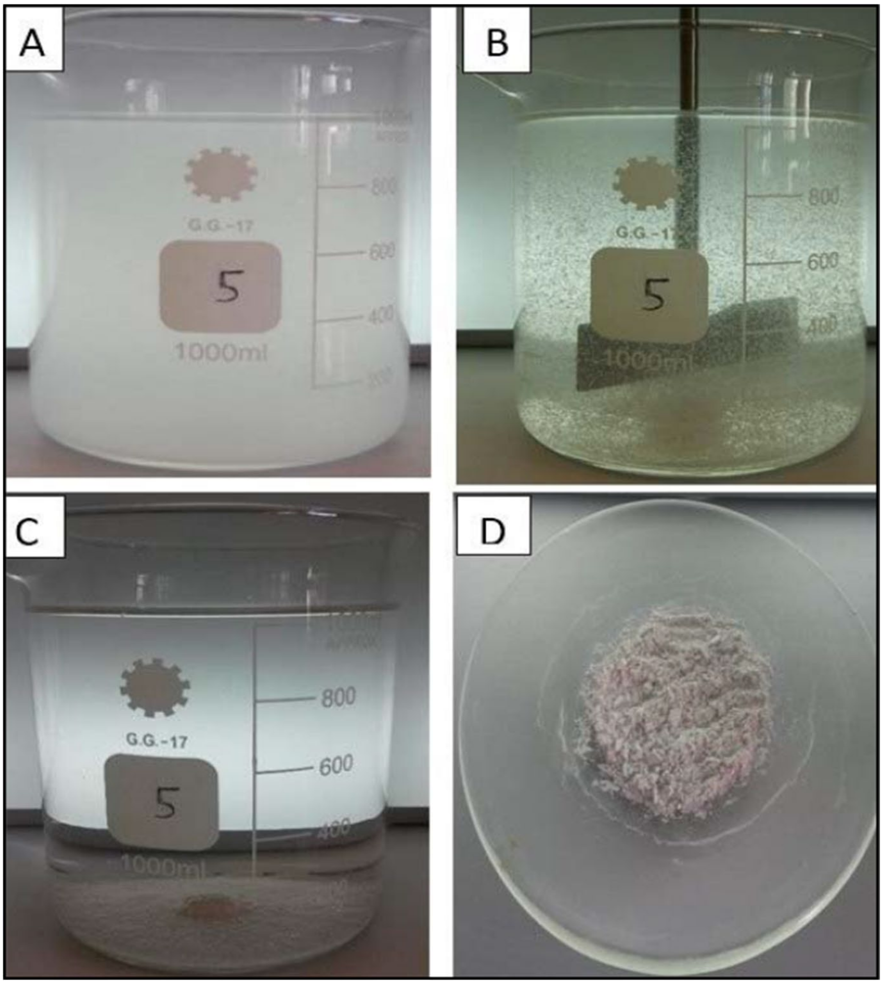

Fig. 2 **A** Raw water sample with initial turbidity of 100 NTU with 110 mg. L^{-1} of MOSE. **B** Aggregation of particles in flocculation step. **C** Settlement of flocs after 25 min. **D** dried solid flocs

NTU was placed individually in a beaker. The water samples were allowed to settle down for 60 min. Samples were collected each 10 min from the surface of the water in the beakers to measure turbidity. Therefore, the natural sedimentation of kaolin colloidal particles should be deducted from the actual performance efficiency computed from Eq. (1) as shown below in Eq. (2):

$$\text{Performance efficiency} = [\frac{\text{Initial turbidity(NTU)} - \text{Residual turbidity (NTU)}}{\text{Initial turbidity(NTU)}} - \text{natural sedimentation}] * 100 \quad (2)$$

2.4 Floc Formation Kinetics

The Brownian motion of colloidal particles manages the process of coagulation at an early stage (Ricordel & Djelal, 2014). The motion weakens when colloidal particles become destabilized and agglomerate to a diameter greater than 1 µm (Ghernaout et al., 2015). The colloidal removal kinetic models were studied to examine and explain the flocculation mechanisms between the kaolin suspension and the component of MOSE. Kinetic studies were conducted to determine the removal rates and contact periods required to complete the coagulation process (Mohtar et al., 2019). The ability of *M. oleifera* to reduce the turbidity of the water sample is due to their coagulation, such as adsorption and neutralization of the positive charges with colloidal particles in the water (Tunggolou & Payus, 2017). Therefore, the colloidal particle adsorption of *M. oleifera* components U was then calculated using the following equation (Desta & Bote, 2021):

$$U = \frac{V\left(C_o - C_e\right)}{W} \tag{3}$$

where C_o and C_e represent the initial and final concentration of colloidal particles in a water sample, V represents the volume of the suspension sample, and W indicates the MOSE dosage.

2.4.1 Pseudo-First-Order Kinetic Model

Lagergren's first-order expression describes the kinetic aggregation of colloidal particles with the component of MOSE coagulant. The approach is represented by the equation below (Mateus et al., 2018)

$$\log\left(U_e - U_t\right) = \log\left(U_e\right) - \frac{K_1 t}{2.303} \tag{4}$$

where Ut (mg/g) is the floc formation with MOSE component at time t (min) and Ue (mg/g) is the equilibrium colloidal particle aggregated with positive ions in MOSE. The pseudo-first-order rate constant is $k1$ (min^{-1}) (Bekhoukh et al., 2022). A plotting chart of log ($Ue - Ut$) versus t can yield the gradient ($k1$/2.303) and intercept (log Ue). Finally, the equilibrium colloidal particle uptake (Ue) and first-order kinetic constant ($k1$) could be determined.

2.4.2 Model of Pseudo-Second-Order Kinetics

The following equation represents the pseudo-second-order approach. The driving force for transferring colloidal particles ($Ue - Ut$) is proportional to the availability of positive ions in the added dosage of MOSE into the water sample (Bello et al., 2017)

$$\frac{t}{U_t} = \left(\frac{1}{k_2 U_e^2} + \frac{t}{U_e}\right) \tag{5}$$

where k_2 is the second-order rate constant in (L. mg^{-1}·min^{-1}). Slope ($1/U_e$) and intercept $1/(k_2\,U_e{}^2)$ are found from the relationship between t/U_t versus t.

2.5 FTIR Analysis

FTIR characterization was crucial to identify the effective main functional groups; present in the *M. oleifera* seeds that contribute to attracting the colloidal particles in the bulk solution. Seed powders were dried well in an oven set at 50 °C for 2 h. The dried seed was named and delivered to a chemical laboratory for FTIR examination.

2.6 Statistical Analysis

Design expert software (Version 13, Stat-Ease Inc., Minneapolis, USA) was used for the experimental design and analysis of the results. The significance of $p < 0.05$ was considered in all statistical analyses. The significance of ANOVA was used to verify the fitness of the regression model equation. Response surface methodology (RSM) was also applied to determine the effects of the MOSE concentration and initial turbidity variables on the turbidity removal efficiency.

3 Results and Discussion

The characteristics of the tap water used in the experiments are analyzed in the laboratory using the standard method (Federation and Association, 2005) and listed in Table 1.

Table 1 Tap water quality characteristics used for water experiments

No	Parameter	Concentration
1	pH	7.66
2	Turbidity (NTU)	0.46
3	Alkalinity (mg. L^{-1})	186
4	Chloride, Cl^- (mg. L^{-1})	22.1
5	Nitrate, NO_3^- (mg. L^{-1})	3
6	Sulfate, SO_4^{-2}, (mg. L^{-1})	11.84
7	Iron, Fe, (mg. L^{-1})	0.0
8	Calcium, Ca^{+2} (mg. L^{-1})	56.37
9	Magnesium, Mg^{+2} (mg. L^{-1})	29.5
10	Sodium, Na^+(mg. L^{-1})	5.53
11	Conductivity (μS. cm^{-1})	320
12	Potassium, K^+ (mg. L^{-1})	0.94
13	Dissolved oxygen (mg. L^{-1})	5.12

Table 2 The main physical properties of MOSE

Properties	MOSE extract
Appearance	Clear yellow
Turbidity (NTU)	22
Electrical Conductivity (µS.cm^{-1})	795
Specific gravity	0.98
Viscosity (m. Pa/s)	1.086
pH	5.96
Alkalinity (mg. L^{-1} as $CaCO_3$)	28

Table 3 Chemical composition of *M. oleifera* seed powder

Compounds	Weight %	Elements	Weight %
SO_3	6.214	Cu	0.00106
P_2O_5	1.643	Zn	0.00545
K_2O	0.9871	Ni	0.00073
MgO	0.5613	Mn	0.00192
CaO	0.2542	Cr	0.00022
Na_2O	0.157	Co	0.00005
Al_2O_3	0.1076	Se	0.00015
Fe_2O_3	0.03088	Ti	0.00102
Cl	0.02729	V	0.00018
SiO_2	< 0.0016	Br	0.000286

The main physical properties of the prepared MOSE were tested in the laboratory, as shown in Table 2. To identify the chemical composition that formulated the solid seed coagulant structure, the XRF (X-ray fluorescence, Spectro IQ11/Ametek, materials analysis division/Germany) technique scan was used (Mohseni-Bandpei et al., 2018). The results illustrated in Table 3 show that the chemical oxides of SO_3, P_2O_5, K_2O, MgO, CaO, Na_2O, and Al_2O_3 hold the highest percentages (6.214%, 1.643%, 0.9871%, 0.5613%, 0.2542%, 0.157%, and 0.1076%) respectively per 5 g of the seed powder. These functional chemicals give better attraction properties for enhancing the destabilization of colloidal particles from bulk liquid.

Table 3 shows the characteristics of the MOSE coagulant examined by the XRF technique confirming that MOSE is rich with numerous positive multivalent ions. The coagulant has the potential capability to destabilize the particles in turbid water through interparticle bridging. This improves the treatability performance by increasing the agglomeration capacity of floc production during the procedures (Faye et al., 2017; Ribeiro et al., 2019).

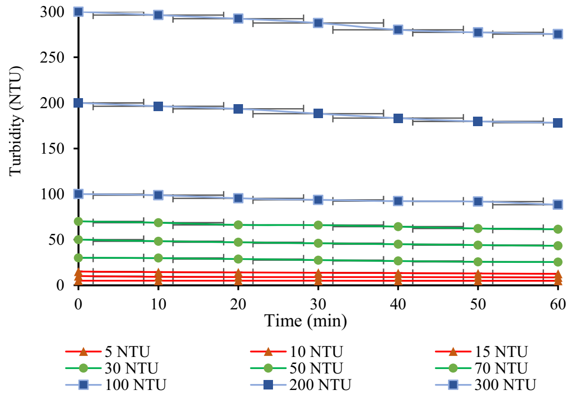

Fig. 3 Natural sedimentation (no coagulant added) of colloidal particles of kaolin in tap water for low, medium, and high initial turbidity

Figure 3 illustrates that the settling velocity of colloidal particles was slow in the absence of a MOSE coagulant. As a consequence, removing turbidity from water is exceptionally difficult and could not achieve the treatment goals. Because of the presence of ions in the tap water quality, the colloidal settlement was consistent with the compression layer settling. An optimum dose of MOSE should be applied to destabilize and neutralize the negative charge of particles causing floc formations to improve the particle settling rate. Thus, acceptable turbidity removal could be achieved.

The coagulation efficiency of MOSE for removing colloidal particles varies depending on the initial turbidity of water and the concentration of the added coagulant extract, as shown in Tables 4, 5, and 6. The performance efficiency of colloidal particles in the three tables was evaluated by considering the decrease in turbidity in the negative control. The investigation showed that the optimum dose for each turbidity range was essential because an overdose of the extract reduced the treatability performance and negatively affected the coagulation treatment process (Zhao et al., 2021). This caused a low reduction in colloidal removal due to the reversed net charge on the suspended solid particles in water (Nkalane et al., 2019). Furthermore, this overdosing resulted in the saturation of the polymer bridge sites and caused the re-stabilization of the particles due to insufficient particles to form more interparticle bridges (Muyibi & Evison,

Table 4 The effect of variation of MOSE dosages on low water turbid removal efficiency at 30 °C

Initial turbidity		5 NTU	Initial turbidity		10 NTU	Initial turbidity		15 NTU
pH before treatment		8.5	pH before treatment		8.5	pH before treatment		8.5
PH after treatment		8.4	pH after treatment		8.3	pH after treatment		8.3
Dosage (mg. L^{-1})	Residual turbidity (NTU)	Removal efficiency (%)	Dosage (mg. L^{-1})	Residual turbidity (NTU)	Removal efficiency (%)	Dosage (mg. L^{-1})	Residual turbidity (NTU)	Removal efficiency (%)
5	4.3±0.15	11.6±0.47	10	6.5±0.25	19.7±0.35	20	8.5±0.13	27.07±0.55
10	4.2±0.10	13.2±0.32	20	6.2±0.20	22.6±0.47	30	8.6±0.18	25.87±0.48
15	4.1±0.20	14.2±0.20	30	5.9±0.15	25.0±0.34	40	8.2±0.11	29.07±0.36
20	4.1±0.25	15.0±0.13	40	5.9±0.10	25.2±0.17	50	6.9±0.20	37.53±0.51
25	4.3±0.35	11.0±0.16	50	5.8±0.20	27.2±0.34	60	6.2±0.15	42.33±0.41
30	4.4±0.30	9.8±0.42	60	5.9±0.22	25.6±0.51	70	6.3±0.23	41.27±0.30

Table 5 The effect of variation of MOSE dosages on medium water turbid removal efficiency at 30 °C

Initial turbidity		30 NTU	Initial turbidity		50 NTU	Initial turbidity		70 NTU
pH before treatment		8.5	pH before treatment		8.5	pH before treatment		8.5
pH after treatment		8.4	pH after treatment		8.3	pH after treatment		8.3
Dosage (mg. L^{-1})	Residual turbidity (NTU)	Removal efficiency (%)	Dosage (mg. L^{-1})	Residual turbidity (NTU)	Removal efficiency (%)	Dosage (mg. L^{-1})	Residual turbidity (NTU)	Removal efficiency (%)
10	22.2±0.73	10.70±0.87	20	20.3±0.93	45.86±0.68	40	9.7±0.54	73.82±0.92
15	19.8±0.98	18.70±0.58	30	18.4±0.65	49.66±0.35	50	6.8±0.48	78.00±0.77
20	15.2±0.45	34.03±0.81	40	16.4±0.20	53.66±0.95	60	6.5±0.07	78.30±0.66
30	12.6±0.39	42.07±0.64	50	14.4±0.60	57.66±0.66	70	6.3±0.05	78.07±0.24
40	4.2±0.40	64.03±0.91	60	4.4±0.45	67.26±0.41	80	3.8±0.20	79.66±0.51
50	6.6±0.22	62.83±0.32	70	12.1±0.27	62.26±0.61	90	9.6±0.30	73.87±0.55

Table 6 The effect of variation of MOSE dosages on high water turbid removal efficiency at 30 °C

Initial turbidity		100 NTU	Initial turbidity		200 NTU	Initial turbidity		300 NTU
pH before treatment		8.5	pH before treatment		8.5	pH before treatment		8.5
PH after treatment		8.4	pH after treatment		8.3	pH after treatment		8.3
Dosage (mg. L^{-1})	Residual turbidity (NTU)	Removal efficiency (%)	Dosage (mg. L^{-1})	Residual turbidity (NTU)	Removal efficiency (%)	Dosage (mg. L^{-1})	Residual turbidity (NTU)	Removal efficiency (%)
80	6.3±0.92	81.95±0.79	180	9.5±0.41	84.4±0.97	190	32.7±0.81	85.61±0.89
90	5.6±0.15	82.68±0.12	190	6.3±0.57	86.0±0.83	200	26.2±0.67	86.73±0.59
100	5.1±0.25	83.14±0.45	200	4.0±0.33	87.1±0.33	210	9.1±0.10	88.78±0.22
110	4.7±0.39	83.53±0.71	210	6.7±0.37	85.8±0.79	220	10.7±0.13	88.25±0.16
120	5.6±0.10	82.61±0.18	220	8.5±0.56	85.0±0.34	230	8.1±0.12	89.14±0.56
130	7.6±0.53	80.69±0.85	230	13.4±0.42	82.4±0.58	240	12.6±0.30	87.62±0.94

1996). Therefore, these three tables' results confirmed that increasing the coagulant dosage enhances treatability performance until agglomeration saturation is reached, whereby the performance starts to decline or stabilize. It was also demonstrated that tap water's ionic composition greatly impacted the sorption of MOSE by colloidal particles or the configuration of the coagulant at the particle–water interface. Optimum doses of MOSE were investigated for different initial turbidity to give minimum residual turbidity. Tables 4, 5, and 6 illustrate that the optimum dose concentration of MOSE to reduce the initial turbidity of water samples 5, 10, 15, 30, 50, 70, 100, 200, and 300 NTU were 20, 50, 60, 40, 60, 80, 110, 200, and 230 mg. L^{-1} respectively with $p<0.05$. As the initial turbidity of the water sample was increased, the required optimum dosage of MOSE also increased. The results of the effect of the initial turbidity on the turbidity reduction by MOSE are shown in Fig. 4. It was also observed that MOSE coagulant showed an exceptional performance efficiency reaching 89% ± 0.56, 80% ± 0.51, and 42% ± 0.41 for high, medium, and low initial turbidity of water samples, respectively. This confirmed the removal efficiency of water turbidity samples with *M. oleifera* coagulant is increased when water comes with dense suspended particles. However, its effectiveness declines with low turbid water. The reason is that the amount of oil in the seed extract forms a film coating that inhibits contact with the surface of the reaction and thus causes the formation of low-strength flocs (Muyibi et al., 2002).

All the experimental results in Tables 4, 5, and 6 revealed that the optimum dosage of *M. oleifera* seeds that gave the lowest residual turbidity depended on the water sample's initial turbidity. Furthermore, when MOSE concentration exceeds the optimum dosage, the turbidity of water increases because all colloids have been neutralized and settled down with an optimum dosage. Thus, the excess coagulants cause turbidity in the water as they do not interact with oppositely charged colloidal particles (Shaarani et al., 2019).

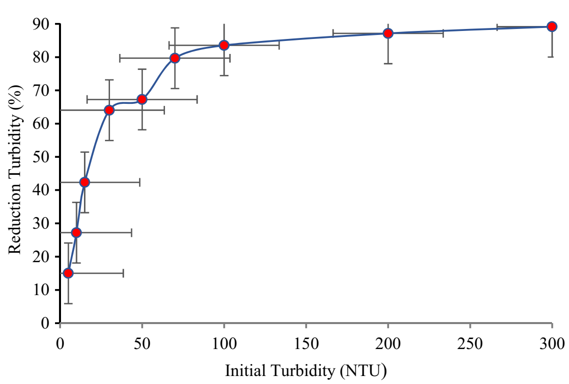

Fig. 4 Turbidity reduction efficiency of MOSE for different initial turbidity of water at optimum dosage

The variables affecting the coagulation process were analyzed using response surface methodology (RSM). The variation of processing factor of both initial water turbidity and added MOSE concentration on turbidity reduction was investigated. Fifty-four experiment runs were generated using central composite design (CCD) during the analysis through Design-Expert software. The method of coding the variables of initial turbidity X_1 and MOSE dosage concentration X_2 was identified as reported in Table 7.

In the study, the removal efficiency response of MOSE Y after the coagulation process was correlated with both independent variables of X_1 and X_2 in a quadratic regression model, as presented in Eq. 6. The significance of these two variables on the removal efficiency was evaluated, as shown in Table 8. It is noted that the X_1 and X_2 indicate the linear coefficient and effect of individual factor separately, whereas the variable X_1X_2 represent the interaction between those two factors, while the second-order terms $X_1{}^2$ and $X_2{}^2$ indicate their quadratic effects. The positive and negative signs indicate synergistic and antagonistic effects of the terms, respectively. The ANOVA result analysis in Table 8 shows that the regression model was significant, with an F-value of 99.26 and having a corresponding low p-value ($p<0.0001$). The value of determination coefficient R^2 of 0.9118 was achieved for the regression equation model which revealed a good fit for the experimental resulted data.

$$Y = 6.57675 + 0.404573X_1 + 0.047671X_2 + 1.395 * 10^{-3}X_1X_2 - 1.313 * 10^{-3}X_1^2 - 2.12 * 10^{-3}X_2^2 \quad (6)$$

Table 7 Experimental factor codes and levels

Variables	Symbol	Coded Variable levels		
		−1	0	+1
Initial turbidity (NTU)	X_1	5	152.5	300
MOSE dosage (mg. L^{-1})	X_2	5	122.5	240

Table 8 ANOVA test for response surface quadratic model

Source	DF	Sum of squares	Mean square	*F*-Value	*P*-Value
Model	5	61,134.7	12,226.94	99.26	< 0.0001
X_1 (NTU)	1	20,792.5	20,792.5	168.79	< 0.0001
X_2 (mg. L^{-1})	1	12,609.96	12,609.96	102.36	< 0.0001
X_1*X_2	1	14,032.14	14,032.14	113.91	< 0.0001
$(X_1)^2$	1	14,174.76	14,174.76	115.07	< 0.0001
$(X_2)^2$	1	14,829.89	14,829.89	120.39	< 0.0001
Residual	48	5912.98	123.19		
Lack of fit	3	5912.98	1970.99		
Pure error	45	0.0000	0.0000		
Cor total	53	67,047.67	R^2	0.9118	
Std. dev		11.1	Adjusted R^2	0.9026	
Mean		52.86	Predicted R^2	0.8892	
C.V.%		21	Ad. Precision	27.067	

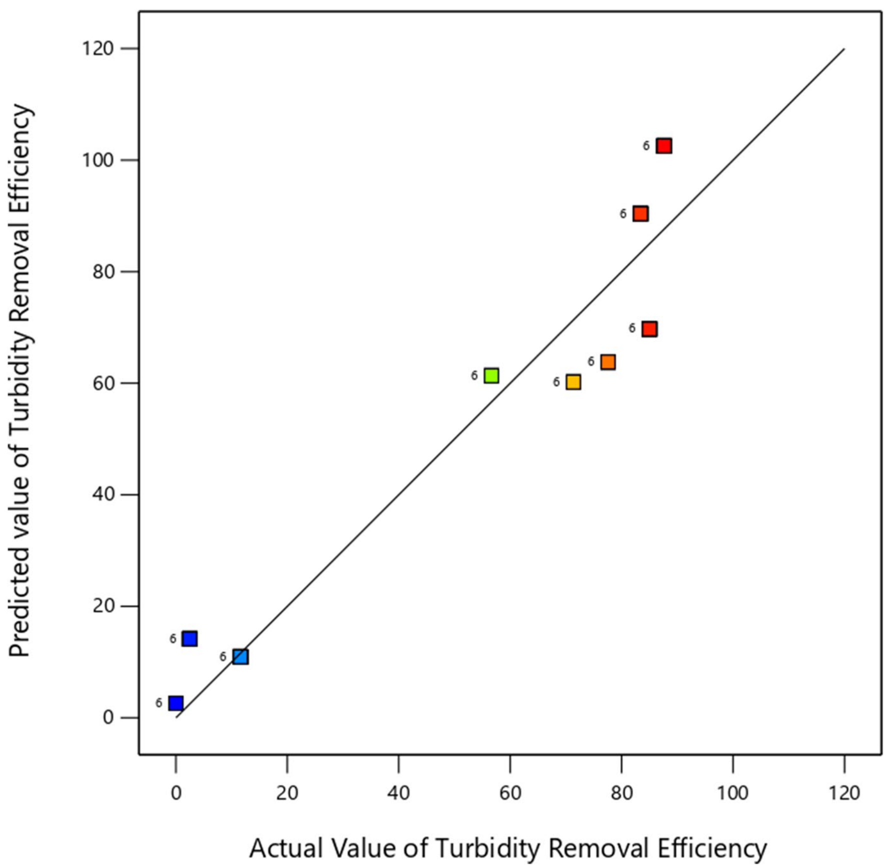

Fig. 5 Actual and predicted value plot for the turbidity removal efficiency of water samples

The low values of residual in Table 8 showed that the model fit was satisfactory, implying that approximately 90% of the dependent variable variance was ascribed to the independent factors and only around 10% of the overall variation could not be explained by the model. Furthermore, it is clear in the Table that the lack-of-fit term is not significant, the difference between adjusted and predicted R^2 is less than

0.2, and the adequate signal-to-noise ratio is greater than 4 indicating that the model is significant. As a result, the developed model can be used to make theoretical predictions for the dependent variable of removal efficiency.

Figure 5 shows the correlation between the observed and predicted values obtained from the software. The figure also illustrates the residual typical plot, which reveals that the model has a few deviations from normal, suggesting a good fit. The figure clearly shows that all data points are distributed and very close along the 45-degree straight line, implying that the proposed quadratic model can positively predict removal efficiency response over independent variable inputs.

Figure 6 illustrates a design expert surface plot exhibiting initial turbidity and MOSE dosage interaction effects on water turbidity decrease. The figure shows that initial water turbidity and MOSE concentration significantly impact the percentage removal rate of colloidal particles in water samples. In low-range turbidity, the dosage of MOSE is not potentially effective to achieve high removal efficiency. The figure also shows that over-dosing MOSE on low-range turbidity samples results in a lower reduction in removal rate due to the reversed net charge on the colloidal particles in water. Consequently, the excess dose has a negative impact on the coagulation treatment process, resulting in a poor reduction of colloidal removal. However, a steep increase in removal efficiency was noticed when the high initial turbidity of samples was treated with an adequate dosage of MOSE.

To improve coagulation, and achieve more efficient removal for low turbidity water, bioactive elements such as seed oil content were isolated and the active constituents of the extract were used (Vilaseca et al., 2014) as the results are shown in Table 9. The residual turbidity of water in this investigation can be further reduced if water flows through a filtration unit like a sand filter, it is easy for the community in rural areas to build such a filter unit. In the experiment tests, MOSE has been found as a potential clarifying agent in water treatment to neutralize and adsorb suspended particles present in the water.

In the experiment runs, no pH adjustment was carried out for the prepared initial samples as with MO coagulant there is no possibility of enhanced hydrophilicity as well as a reduction in the charge neutralization of the water molecules. This affirmed

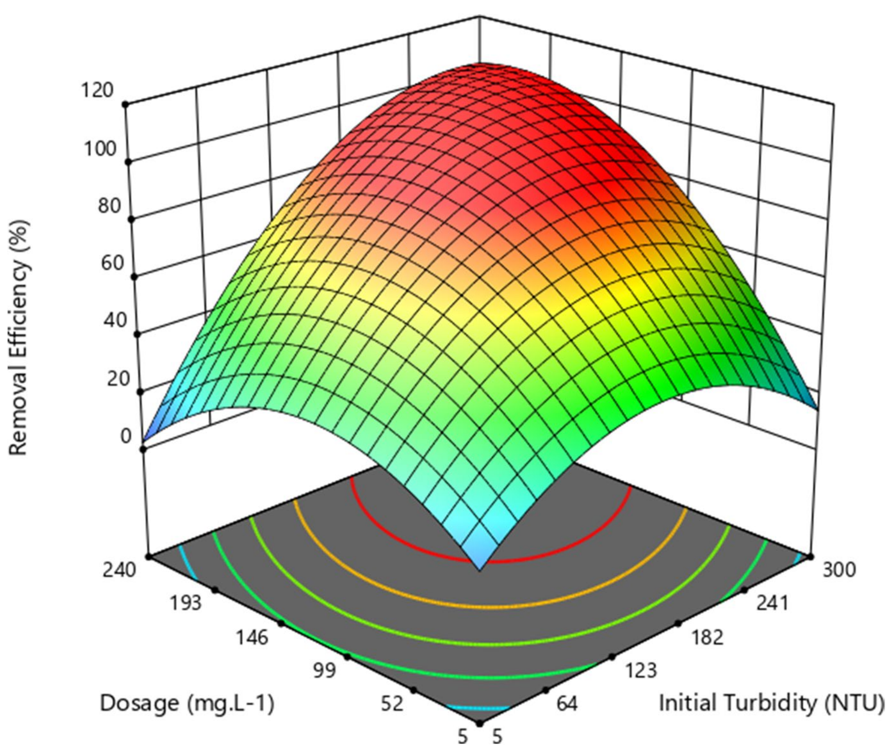

Fig. 6 Design expert surface plot showing the interaction effects of both initial turbidity and MOSE dosage on the reduction of water turbidity

Table 9 The effect of de-oiled MOSE dosages on low water turbid removal efficiency at 30 °C

Initial turbidity		5 NTU	Initial turbidity		10 NTU	Initial turbidity		15 NTU
pH before treatment		8.5	pH before treatment		8.5	pH before treatment		8.5
PH after treatment		8.4	pH after treatment		8.3	pH after treatment		8.3
Dosage (mg. L^{-1})	Residual turbidity (NTU)	Removal efficiency (%)	Dosage (mg. L^{-1})	Residual turbidity (NTU)	Removal efficiency (%)	Dosage (mg. L^{-1})	Residual turbidity (NTU)	Removal efficiency (%)
10	1.63 ± 0.10	64.4 ± 0.35	15	1.85 ± 0.35	66.0 ± 0.24	20	2.13 ± 0.22	69.2 ± 0.24
15	1.45 ± 0.25	68.0 ± 0.32	20	1.72 ± 0.31	67.5 ± 0.12	25	1.78 ± 0.24	71.5 ± 0.35
20	1.26 ± 0.20	71.8 ± 0.15	25	1.42 ± 0.25	70.5 ± 0.25	30	1.49 ± 0.35	73.5 ± 0.12
25	1.06 ± 0.35	75.8 ± 0.11	30	1.23 ± 0.20	72.4 ± 0.10	35	1.27 ± 0.15	75.0 ± 0.10
30	1.18 ± 0.35	73.4 ± 0.10	35	1.51 ± 0.10	69.6 ± 0.10	40	1.24 ± 0.16	75.1 ± 0.15
35	1.27 ± 0.12	71.6 ± 0.21	40	1.59 ± 0.10	68.8 ± 0.16	45	1.31 ± 0.10	74.7 ± 0.20

coalescing ability and electrostatic attraction between water and MOSE coagulant. Therefore, the treatability performance of the MOSE coagulant was not dependent on the pH value of the water solution (Shan et al., 2017). Tables 4, 5, 6, and 7 illustrate that the water solutions' pH value before and after the experiments was quite stable. A similar result was obtained by Nhut et al. (2021).

In the investigation, it was observed that turbidity reduction with the application of MOSE improves agglomeration performance. The growth of flocs and agglomeration in the flocculation part was promoted, increasing the removal of colloidal matter in water. This is attributed to an enhancement in the floc size, with the performance of the coagulant in turbidity removal causing the rapid settling ability of the flocs due to coalescing of the colloids formed in suspension (Adelodun et al., 2020). Thus, the extent of aggregation and flocculation dynamics of colloidal particles in the experiments were observed shortly after the addition of the coagulants, whereby the destabilized particles aggregated to form larger flocs.

To understand the coagulation-flocculation kinetics, the extent of aggregation was monitored. This was carried out by investigating the effect of sedimentation time 45 min at a dosage of 50 mg. L^{-1}—10 NTU, 60 mg. L^{-1}—50 NTU, 210 mg. L^{-1}—200 NTU. It was noticed that the concentration of colloidal solids decreased as the time of treatment increased. Figure 7 reveals that the optimum settling time to achieve turbidity removal efficiency for each run in the experimental tests was 30 min. This duration time for settling the floc formations is convenient and desirable

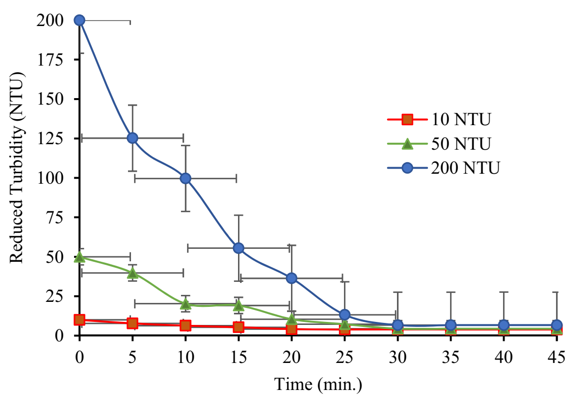

Fig. 7 Turbidity-time decay curves for three different initial turbidities of water at a convenient dosage of MOSE

due to the energy and time savings. Furthermore, a real clarification in water was noticed due to the activity of the extract with an increase in the settling time specifically at the beginning of the process.

The data for water turbidity reduction with respect to time for three ranges 10, 50, 200)NTU was fitted to kinetic Eqs. 4 and 5 to illustrate the best kinetic model in the removal of colloidal particles in water to form flocs as shown in Fig. 8. The resulting data were best fitted to a pseudo-first-order kinetic model with a high determinant coefficient, as shown in Table 10. A similar result was obtained by Ruelas-Leyva et al. (2017). The colloidal removal rate in the reaction kinetic is based on numerous internal and external factors such as dosage, and the characteristics of the water itself (Precious Sibiya et al., 2021). As the reaction proceeds,

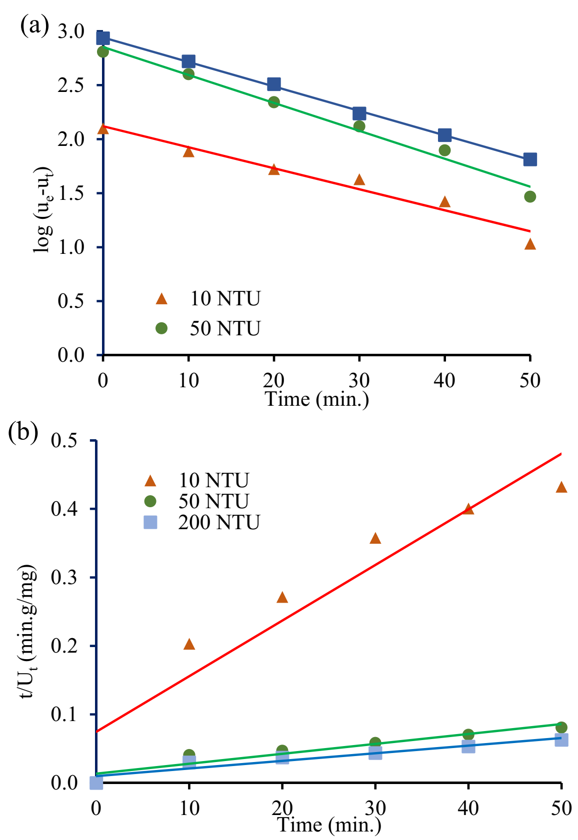

Fig. 8 Fitting kinetic experimental data of three different raw water with models of a pseudo first order and **b** pseudo second order

particles adhere themselves to both chemical and physical binding sites. The reaction lasts until the free sites are completely saturated, with rapid settling at first.

Some physicochemical parameters for raw turbid water 100 NTU were measured before and after treatment with an optimum dosage of MOSE to reveal the extent of variation of water characteristics when treated with MOSE coagulant. The experimental results and ANOVA statistical analysis as shown in Tables 11 and 12 demonstrated that the treatment of water with crude MOSE showed little change in pH, electrical conductivity, and salinity. However, the alkalinity and hardness of water significantly decreased depending on the initial hardness and the added MOSE dosage ($p < 0.05$). This result was consistent with what was found by Muyibi and Evison (1996).

Colloidal particle aggregation in turbid water is mainly based on the surface chemistry of MOSE (Araujo et al., 2010). Transmission FTIR spectra for the *Moringa oleifera* solid particle were obtained for identifying the effective surface functional groups as depicted in Fig. 9. The detected bands of 2856, 2926, and 3288 cm^{-1} are assigned to –OH stretching (Ogunmodede et al., 2021). The broad band centered at 3420 cm^{-1} is assigned to O–H stretching. The FTIR spectra of the seed showed a broad range of frequency approximately between 1666–2856 cm^{-1} and 3288–4000 representing the existence of free hydroxyl groups and bonded –OH bands of carboxylic acids. The sharp bending modes at peaks of 1666, 1542, 1239, and 1058 cm^{-1} are assigned to vibrations of groups. This functional group appears predominantly in the protein and fatty acid structures present in *Moringa* seeds. The peaks at 2923 cm^{-1} and 2852 cm^{-1} are assigned to symmetrical and asymmetrical stretching of the C–H of CH_2 group present in fatty acids (Kizilkaya & Tekınay, 2014). In the region between 1666 and 1058 cm^{-1}, there are intense bands assigned to C = O bond stretching. The spectra show the band at 1666 cm^{-1} associated with the amide group in the protein and the presence of a peak at 1542 cm^{-1} is assigned to C = N stretching and/or N–H deformation (Kizilkaya & Tekınay, 2014).

Table 10 Kinetic model parameters for water samples treated with MOSE at 30 °C

Models	Parameter	10 NTU	50 NTU	200 NTU
Pseudo-first order	K_1 (min^{-1})	0.045	0.0596	0.0522
	U_e	132	713.02	876
	R^2	0.9564	0.9844	0.9988
Pseudo-second order	K_2 ($L.mg^{-1}{\cdot}min^{-1}$)	8.77E-04	1.463E-04	1.22E-04
	U_e	123.46	714.29	909.1
	R^2	0.8993	0.9040	0.9119

Table 11 Some physicochemical parameters at optimum dosage of MOSE for raw turbid water 100 NTU

No	Parameters	Unit	Untreated water	Results				
				90 (mg. L^{-1})	100 (mg. L^{-1})	110 (mg. L^{-1})	120 (mg. L^{-1})	130 (mg. L^{-1})
1	Turbidity	NUT	100	5.57	5.11	4.72	5.64	7.56
2	Temperature	°C	32	32	32	32	32	32
3	pH		7.5	7.4	7.5	7.4	7.4	7.5
4	E.C	μS/cm	420	421	423	424	426	427
5	Salinity	(mg. L^{-1})	268.8	270.08	272.3	273.4	275.6	276.31
6	Alkalinity	(mg. L^{-1}) as $CaCO_3$	230.21	226.11	220.12	216.00	213.02	208.13
7	Hardness	(mg. L^{-1}) as $CaCO_3$	220	220.8	214	211	208	206.76

Table 12 ANOVA test for physiochemical properties of turbid water 100 NTU coagulated with MOSE

Properties	Source	Sum of squares	Mean square	*F*-Value	*P*-Value	
pH	X_1	9.5 E-03	9.5 E-03	0.19	0.702	Not significant
	X_2	1.22 E-03	1.22 E-03	0.25	0.667	Not significant
E.C	X_1	3.47	3.47	10.06	0.087	Not significant
	X_2	3.38	3.38	9.81	0.089	Not significant
Salinity	X_1	10.59	10.59	0.71	0.488	Not significant
	X_2	230.6	230.6	15.5	0.059	Not significant
Alkalinity	X_1	4.815	4.815	20.57	0.045	Significant
	X_2	277.97	277.97	1187.23	0.001	Significant
Hardness	X_1	14.4	14.4	19.29	0.048	Significant
	X_2	110.89	110.89	148.56	0.007	Significant

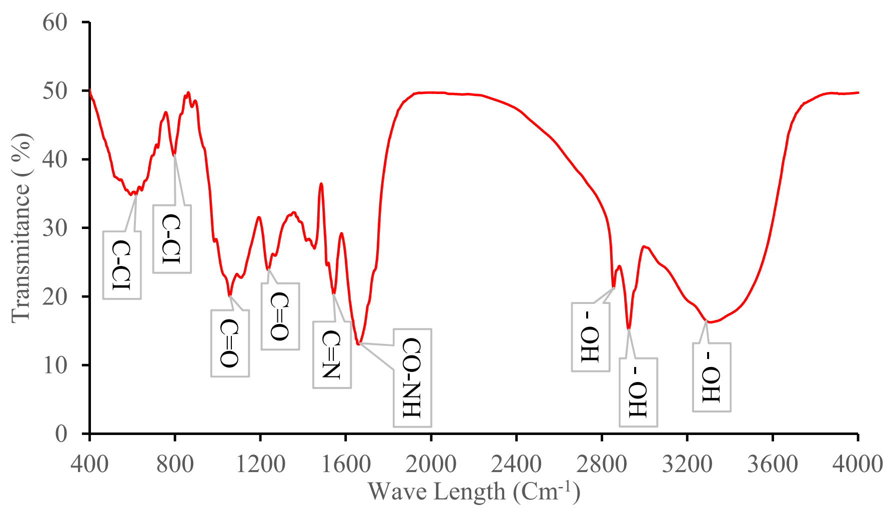

Fig. 9 FT-IR spectrum of *Moringa oleifera* seeds, the maximum and minimum peaks obtained is shown in the boxes

4 Conclusions

The *M. oleifera* plant has a rapid growth rate with less duration time in rural areas, a simple technique to use its extract, and unskilled persons can easily and effectively employ this natural material without facing problems. Therefore, the coagulant of MOSE is locally available in large volumes and is feasibly economical. The results strongly supported the efficacy of *M. oleifera* as a better alternative to synthetic coagulants in water purification. The optimum MOSE dosage for the coagulation-flocculation process varies based on the initial water turbidity. Therefore, the high turbidity removal achieved in this study confirmed the potential of this important eco-friendly natural product potential for safely treating water in rural regions.

Acknowledgements The authors are thankful to the college of engineering at the University of Sulaymaniyah, Iraq, for their support and analytical test services. Also, financial support from the same university was most helpful in achieving this work.

Funding Open access funding provided by Lulea University of Technology.

Data Availability The datasets generated during and/or analyzed during the current study are available from the corresponding author on reasonable request.

Declarations

Conflict of Interest The authors declare no competing interests.

References

Adelodun, B., Ogunshina, M. S., Ajibade, F. O., Abdulkadir, T. S., Bakare, H. O., & Choi, K. S. (2020). Kinetic and prediction modeling studies of organic pollutants removal from municipal wastewater using Moringa oleifera biomass as a coagulant. *Water, 12*(7), 2052. https://doi.org/10.3390/w12072052

Ang, W. L., & Mohammad, A. W. (2020). State-of-the-art and sustainability of natural coagulants in water and wastewater treatment. *The Journal of Cleaner Production, 262*, 121267. https://doi.org/10.1016/j.jclepro.2020.121267

Anthony, E. T., Ojemaye, M. O., Okoh, A. I., & Okoh, O. O. (2021). Potentials of low-cost methods for the removal of antibiotic-resistant bacteria and their genes in low-budget communities: A review The Journal of Water. *Process Engineering, 40*, 101919. https://doi.org/10.1016/j.jwpe.2021.101919

Araujo, C. S., Alves, V. N., Rezende, H. C., Almeida, I. L., de Assunçao, R. M., Tarley, C. R., & Coelho, N. M. M. (2010). Characterization and use of Moringa oleifera seeds as biosorbent for removing metal ions from aqueous effluents. *Water Science and Technology, 62*(9), 2198–2203. https://doi.org/10.2166/wst.2010.419

Bekhoukh, A., Moulefera, I., Zeggai, F. Z., Benyoucef, A., & Bachari, K. (2022). Anionic methyl orange removal from aqueous solutions by activated carbon reinforced conducting polyaniline as adsorbent: Synthesis, characterization, adsorption behavior, regeneration, and kinetics study. *Journal of Polymers and the Environment, 30*(3), 886–895. https://doi.org/10.1007/s10924-021-02248-6

Bello, O. S., Lasisi, B. M., Adigun, O. J., & Ephraim, V. (2017). Scavenging Rhodamine B dye using Moringa oleifera seed pod. *Chemical Speciation & Bioavailability, 29*(1), 120–134. https://doi.org/10.1080/09542299.2017.1356694

Bhatia, S., Othman, Z., & Ahmad, A. L. (2007). Pretreatment of palm oil mill effluent (POME) using Moringa oleifera seeds as a natural coagulant. *Journal of Hazardous Materials, 145*(1–2), 120–126. https://doi.org/10.1016/j.jhazmat.2006.11.003

Cui, H., Huang, X., Yu, Z., Chen, P., & Cao, X. (2020). Application progress of enhanced coagulation in water treatment. *RSC Advances, 10*(34), 20231–20244. https://doi.org/10.1039/D0RA02979C

Desta, W. M., & Bote, M. E. (2021). Wastewater treatment using a natural coagulant (Moringa oleifera seeds) Optimization through response surface methodology. *Heliyon, 7*(11), e08451. https://doi.org/10.1016/j.heliyon.2021.e08451

Dzuvor, C. K., Pan, S., Amanze, C., Amuzu, P., Asakiya, C., & Kubi, F. (2022). Bioactive components from Moringa oleifera seeds: Production, functionalities, and applications–a critical review. *Critical Reviews in Biotechnology, 42*(2), 271–293. https://doi.org/10.1080/07388551.2021.1931804

El-Hack, A., Mohamed, E., Alagawany, M., Elrys, A. S., Desoky, E. S. M., Tolba, H., & Swelum, A. A. (2018). Effect of forage Moringa oleifera L (moringa) on animal health and nutrition and its beneficial applications in soil, plants and water purification. *Agriculture, 8*(9), 145. https://doi.org/10.3390/agriculture8090145

Elsayed, E. M., Nour El-Den, A. A., Elkady, M. F., & Zaatout, A. A. (2021). Comparison of coagulation performance using natural coagulants against traditional ones. *Separation Science and Technology, 56*(10), 1779–1787. https://doi.org/10.1080/01496395.2020.1795674

Faye, M. C. A. S., Zhang, Y., & Yang, J. (2017). Extracellular polymeric substances and sludge solid/liquid separation under Moringa oleifera and chitosan conditioning: A review. *Environ Tech Rev, 6*(1), 59–73. https://doi.org/10.1080/21622515.2017.1282544

Federation, W. E., & Association, A. P. H. (2005). *Standard methods for the examination of water and wastewater*. American Public Health Association (APHA).

Gaikwad, V. T., & Munavalli, G. R. (2019). Turbidity removal by conventional and ballasted coagulation with natural coagulants. *App Wat Sci., 9*(5), 1–9. https://doi.org/10.1007/s13201-019-1009-6

Gara, T., Fengting, L., Nhapi, I., Makate, C., & Gumindoga, W. (2018). Health safety of drinking water supplied in Africa: A closer look using applicable water-quality standards as a measure. *Expos. Heal., 10*(2), 117–128. https://doi.org/10.1007/s12403-017-0249-7

Ghernaout, D., Al-Ghonamy, A. I., Boucherit, A., Ghernaout, B., Naceur, M. W., Messaoudene, N. A., & Elboughdiri, N. A. (2015). Brownian motion and coagulation process. *American Journal of Environmental Protection, 4*(51), 1–15. https://doi.org/10.11648/j.ajeps.s.2015040501.11

Igwe, P. U., Chukwudi, C. C., Ifenatuorah, F. C., Fagbeja, I. F., & Okeke, C. A. (2017). A review of environmental effects of surface water pollution. *International Journal of Advanced Engineering Research and Science, 4*(12), 237340. https://doi.org/10.22161/ijaers.4.12.21

Jagaba, A. H., Kutty, S. R. M., Hayder, G., Latiff, A. A. A., Aziz, N. A. A., Umaru, I., & Nasara, M. A. (2020). Sustainable use of natural and chemical coagulants for contaminants removal from palm oil mill effluent: A comparative analysis. *Ain Shams Engineering Journal, 11*(4), 951–960. https://doi.org/10.1016/j.asej.2020.01.018

Katrivesis, F. K., Karela, A. D., Papadakis, V. G., & Paraskeva, C. A. (2019). Revisiting of coagulation-flocculation processes in the production of potable water. *Journal of Water Process Engineering, 27*, 193–204. https://doi.org/10.1016/j.jwpe.2018.12.007

Khader EH, Mohammed THJ, and Mirghaffari N (2018) Use of natural coagulants for removal of COD, oil, and turbidity from produced waters in the petroleum industry. Journal of Petroleum & Environmental Biotechnology 9(3). https://doi.org/10.4172/2157-7463.1000374

Kizilkaya B and Tekınay AA (2014). Utilization to remove Pb (II) ions from aqueous environments using waste fish bones by ion exchange. Journal of Chemistry 2014. https://doi.org/10.1155/2014/739273

Krupinska, I. (2020). Aluminium drinking water treatment residuals and their toxic impact on human health. *Mole, 25*(3), 641. https://doi.org/10.3390/molecules25030641

Kurniawan, T. A., Sillanpaa, M. E., & Sillanpaa, M. (2012). Nano adsorbents for remediation of aquatic environment: Local and practical solutions for global water pollution problems. *Critical Reviews in Environmental Science and Technology, 42*(12), 1233–1295. https://doi.org/10.1080/10643389.2011.556553

Leone, A., Spada, A., Battezzati, A., Schiraldi, A., Aristil, J., & Bertoli, S. (2016). Moringa oleifera seeds and oil: Characteristics and uses for human health. *International Journal of Molecular Sciences, 17*(12), 2141. https://doi.org/10.3390/ijms17122141

Mateus GAP, Dos Santos TRT, Sanches IS, Silva MF, de Andrade MB, Paludo MP, ... and Bergamasco R (2018). Evaluation of a magnetic coagulant based on Fe3O4 nanoparticles and Moringa oleifera extract on tartrazine removal: Coagulation-adsorption and kinetics studies. Environmental Technology 41(13):1–42. https://doi.org/10.1080/09593330.2018.1543358.

Matta, G., Srivastava, S., Pandey, R. R., & Saini, K. K. (2017). Assessment of physicochemical characteristics of Ganga Canal water quality in Uttarakhand. *Environment, Development and Sustainability, 19*(2), 419–431. https://doi.org/10.1007/s10668-015-9735-x

Mohseni-Bandpei, A., Motesaddi, S., Eslamizadeh, M., Rafiee, M., Nasseri, M., MontazeriNamin, M., & Riahi, S. M. (2018). Water-quality assessment of the most important dam (Latyan dam) in Tehran Iran. *Environmental Science and Pollution Research, 25*(29), 29227–29239. https://doi.org/10.1007/s11356-018-2865-6

Mohtar, S. S., Saman, N., Noor, A. M. M., TengkuMalimBusu, T. N. Z., Yusoff, N. A., & Mat, H. (2019). Flocculation kinetics and dewatering studies of quaternized cellulose derived from oil palm empty fruit bunches. *The Korean Journal of Chemical Engineering, 36*(5), 669–677. https://doi.org/10.1007/s11814-019-0250-x

Moulin, M., Moscou, E., Signor, L., Kieffer-Jaquinod, S., KwaambwaNermark, H. M. F., & Rennie, A. R. (2019). Towards a molecular understanding of the water purification properties of Moringa seed proteins. *Journal of Colloid and Interface Science, 554*, 296–304. https://doi.org/10.1016/j.jcis.2019.06.071

Mumbi, A. W., Fengting, L., & Karanja, A. (2018). Sustainable Treatment of Drinking Water Using Natural Coagulants in Developing Countries: A Case of Informal Settlements in Kenya. *Water Utility Journal*, 18, 1–11.

Muyibi, S. A., & Evison, L. M. (1995). Optimizing physical parameters affecting coagulation of turbid water with Moringa oleiferaseeds. *Water Research, 29*(12), 2689–2695. https://doi.org/10.1016/0043-1354(95)00133-6

Muyibi, S. A., & Evison, L. M. (1996). Coagulation of turbid water and softening of hard water with Moringa oleifera seeds. *International Journal of Environmental Studies, 49*(3), 247–259. https://doi.org/10.1080/00207239608711028

Muyibi, S. A., Mohd Noor, M. J. M., Leong, T. K., & Loon, L. H. (2002). Effects of oil extraction from Moringa oleifera seeds on coagulation of turbid water. *International Journal of Environmental Studies, 59*(2), 243–254. https://doi.org/10.1080/00207230210924

Nan, J., Yao, M., Chen, T., Li, S., Wang, Z., & Feng, G. (2016). Breakage and regrowth of flocs formed by sweep coagulation using additional coagulant of poly aluminum chloride and non-ionic polyacrylamide. *Environmental Science and Pollution Research, 23*(16), 16336–16348. https://doi.org/10.1007/s11356-016-6805-z

Nhut, H. T., Hung, N. T. Q., Lap, B. Q., Han, L. T. N., Tri, T. Q., Bang, N. H. K., & Ky, N. M. (2021). Use of *Moringaoleifera* seeds powder as bio-coagulants for the surface water treatment. *International Journal of Environmental Science and Technology, 18*(8), 2173–2180. https://doi.org/10.1007/s13762-020-02935-2

Nkalane, A., Oyewo, O. A., Leswifi, T., & Onyango, M. S. (2019). Application of coagulant obtained through charge reversal of sawdust-derived cellulose nanocrystals in the enhancement of water turbidity removal. *Materials Research Express,6*(10), 105060. https://doi.org/10.1088/2053-1591/ab3b49

Ogunmodede, J., Akanji, S. B., & Bello, O. S. (2021). Moringa oleifera seed pod-based adsorbent for the removal of paracetamol from aqueous solution A novel approach toward diversification. *Environmental Progress Sustainable Energy, 40*(4), e13615. https://doi.org/10.1002/ep.13615

Precious Sibiya, N., Rathilal, S., & KweinorTetteh, E. (2021). Coagulation treatment of wastewater: Kinetics and natural coagulant evaluation. *Mole., 26*(3), 698. https://doi.org/10.3390/molecules26030698

Rajoria S, Vashishtha M, and Sangal VK (2022) Treatment of electroplating industry wastewater: A review on the various techniques. Environmental Science and Pollution Research 1–51. https://doi.org/10.1007/s11356-022-18643-y

Razali, A., Syed Ismail, S. N., Awang, S., Praveena, S. M., & Zainal Abidin, E. (2020). The impact of seasonal change on river water quality and dissolved metals in mountainous agricultural areas and risk to human health. *Environ Fore, 21*(2), 195–211. https://doi.org/10.1080/15275922.2020.1728434

Ribeiro JVM, Andrade PV, and Reis AGD (2019) *Moringa oleifera* seed as a natural coagulant to treat low-turbidity water by in-line filtration. Revista Ambiente and Água 14. https://doi.org/10.4136/ambi-agua.2442

Ricordel, C., & Djelal, H. (2014). Treatment of landfill leachate with a high proportion of refractory materials by electrocoagulation: System performances and sludge settling characteristics. *Journal of Environmental Chemical Engineering, 2*(3), 1551–1557. https://doi.org/10.1016/j.jece.2014.06.014

Ruelas-Leyva, J. P., Contreras-Andrade, I., Sarmiento-Sánchez, J. I., Licea-Claverie, A., Jimenez-Lam, S. A., Cristerna-Madrigal, Y. G., & Picos-Corrales, L. A. (2017). The effectiveness of Moringa oleifera seed flour and chitosan as coagulant-flocculants for water treatment. *Clean-Soil Air Water, 45*(8), 1600339. https://doi.org/10.1002/clen.201600339

Saravanan, A., Kumar, P. S., Jeevanantham, S., Karishma, S., Tajsabreen, B., Yaashikaa, P. R., & Reshma, B. (2021). Effective water/wastewater treatment methodologies for toxic pollutants removal Processes and applications towards sustainable development. *Chemotherapy, 280*, 130595. https://doi.org/10.1016/j.chemosphere.2021.130595

Saxena, K., Brighu, U., & Choudhary, A. (2018). Parameters affecting enhanced coagulation: A review. *Environmental Technology Reviews, 7*(1), 156–176. https://doi.org/10.1080/21622515.2018.1478456

Shaarani, S., Azizan, S. N. F., Akhir, M. D., Muhammad, F. N., Yuzir, M. A., Othman, N. A., Zakaria, Z., & Hara, H. (2019). The removal efficiency of Gram-positive and Gram-negative bacteria using a natural coagulant during coagulation, flocculation, and sedimentation processes. *Water Science and Technology, 80*(9), 1787–1795. https://doi.org/10.2166/wst.2019.433

Shan, T. C., Matar, M. A., Makky, E. A., & Ali, E. N. (2017). The use of Moringa oleifera seed as a natural coagulant for wastewater treatment and heavy metals removal. *Applied Water Science, 7*(3), 1369–1376. https://doi.org/10.1007/s13201-016-0499-8

Tomperi, J., Isokangas, A., Tuuttila, T., & Paavola, M. (2022). The functionality of turbidity measurement under changing water quality and environmental conditions. *Environmental Technology, 43*(7), 1093–1101. https://doi.org/10.1080/09593330.2020.1815860

Tunggolou, J., & Payus, C. (2017). Moringa oleifera as a coagulant used in the water purification process for consumption. *Earth Sciences Pakistan, 1*(2), 1–3. https://doi.org/10.26480/esp.02.2017.01.03

Vilaseca, M., Lopez-Grimau, V., & Gutierrez-Bouzan, C. (2014). Valorization of waste obtained from oil extraction in Moringa oleifera seeds: Coagulation of reactive dyes in textile effluents. *Materials, 7*(9), 6569–6584. https://doi.org/10.3390/ma7096569

Wu, C., Wang, Y., Gao, B., Zhao, Y., & Yue, Q. (2012). Coagulation performance and floc characteristics of aluminum sulfate using sodium alginate as coagulant aid for synthetic dying wastewater treatment. *Separation and Purification Technology, 95*, 180–187. https://doi.org/10.1016/j.seppur.2012.05.009

Yamaguchi NU, Cusioli LF, Quesada HB, Ferreira ME, Fagundes-Klen MR, Vieira AMS, ... and Bergamasco R (2021). A review of Moringa oleifera seeds in water treatment: Trends and future challenges. Process Safety and Environmental Protection 147: 405–420. https://doi.org/10.1016/j.psep.2020.09.044.

Zhang, C., Zhang, W., Huang, Y., & Gao, X. (2017). Analyzing the correlations of long-term seasonal water quality parameters, suspended solids, and total dissolved solids in a shallow reservoir with meteorological factors. *Environmental Science and Pollution Research, 24*(7), 6746–6756. https://doi.org/10.1007/s11356-017-8402-1

Zhao, C., Zhou, J., Yan, Y., Yang, L., Xing, G., Li, H., & Zheng, H. (2021). Application of coagulation/flocculation in oily wastewater treatment A review. *Science of The Total Environment, 765*, 142795. https://doi.org/10.1016/j.scitotenv.2020.142795